Science
AAAS

Dependence of Olfactory Bulb Neurogenesis on Prokineticin 2 Signaling

Kwan L. Ng, *et al.*

Science **308**, 1923 (2005);
DOI: 10.1126/science.1112103

The changes in synaptic physiology in ErbB-deficient muscles are more subtle than those observed in mice heterozygous for a certain NRG1β isoform (*27*). Because Schwann cells depend on NRG-mediated signaling from motor neurons for survival (*12*), the stronger defects in the NRG1β mutants could be explained by impaired Schwann cell function, which in turn may impair the motor neuron's ability to maintain the synaptic muscle membrane.

Given that NRG is not required for synapse-specific gene transcription at the NMJ, the proposed function of NRG in regulating glutamate receptor expression during synapse development in the brain (*28*) warrants further examination.

References and Notes

1. D. L. Falls, K. M. Rosen, G. Corfas, *Cell* **72**, 801 (1993).
2. L. M. Moscoso *et al.*, *Dev. Biol.* **172**, 158 (1995).
3. M. Rimer *et al.*, *Mol. Cell. Neurosci.* **26**, 271 (2004).
4. E. Tzahar *et al.*, *Mol. Cell. Biol.* **16**, 5276 (1996).
5. S. A. Jo, X. Zhu, M. A. Marchionni, *Nature* **373**, 158 (1995).
6. G. C. Chu, L. M. Moscoso, M. X. Sliwkowski, *Neuron* **14**, 329 (1995).
7. L. Schaeffer, N. Duclert, M. Huchet-Dymanus, *EMBO J.* **17**, 3078 (1998).
8. U. J. McMahan, *Cold Spring Harb. Symp. Quant. Biol.* **55**, 407 (1990).
9. T. M. DeChiara *et al.*, *Cell* **85**, 501 (1996).
10. M. Gautam *et al.*, *Cell* **85**, 525 (1996).
11. A. N. Garratt, S. Britsch, C. Birchmeier, *Bioessays* **22**, 987 (2000).
12. S. Britsch *et al.*, *Genes Dev.* **15**, 66 (2001).
13. M. Leu *et al.*, *Development* **130**, 2291 (2003).
14. H. Tidcombe *et al.*, *Proc. Natl. Acad. Sci. U.S.A.* **100**, 8281 (2003).
15. W. Long *et al.*, *Development* **130**, 5257 (2003).
16. M. Schwander *et al.*, *Dev. Cell* **4**, 673 (2003).
17. P. Escher, H. R. Brenner, unpublished observations.
18. X. Yang *et al.*, *Neuron* **30**, 399 (2001).
19. W. Lin *et al.*, *Nature* **410**, 1057 (2001).
20. A. C. Missias, G. C. Chu, B. J. Klocke, *Dev. Biol.* **179**, 223 (1996).
21. V. Witzemann *et al.*, *Proc. Natl. Acad. Sci. U.S.A.* **93**, 13286 (1996).
22. G. Bezakova, H. R. Brenner, unpublished observations.
23. J. Cossins *et al.*, *Hum. Mol. Genet.* **13**, 2947 (2004).
24. S. Hashemolhosseini *et al.*, *Mol. Cell. Neurosci.* **16**, 697 (2000).
25. T. Meier *et al.*, *J. Neurosci.* **17**, 6534 (1997).
26. M. J. Marques, J. A. Conchello, J. W. Lichtman, *J. Neurosci.* **20**, 3663 (2000).
27. A. W. Sandrock *et al.*, *Science* **276**, 599 (1997).
28. M. Ozaki, M. Sasner, R. Yano, *Nature* **390**, 691 (1997).

29. We thank O. Dorchies (Geneva) for help with myoblast purification and M. A. Ruegg, Y. Barde, and B. Bettler (Basel) for critical comments on the manuscript. This work was supported by the Swiss National Science Foundation, the Swiss Foundation for Research on Muscle Diseases, the Novartis Foundation for Medicine and Biology, and NIH.

Supporting Online Material

www.sciencemag.org/cgi/content/full/308/5730/1920/DC1
Materials and Methods
SOM Text
Figs. S1 to S5
References and Notes

3 December 2004; accepted 25 April 2005
10.1126/science.1108258

Dependence of Olfactory Bulb Neurogenesis on Prokineticin 2 Signaling

Kwan L. Ng, Jia-Da Li, Michelle Y. Cheng, Frances M. Leslie, Alex G. Lee, Qun-Yong Zhou*

Neurogenesis persists in the olfactory bulb (OB) of the adult mammalian brain. New interneurons are continually added to the OB from the subventricular zone (SVZ) via the rostral migratory stream (RMS). Here we show that secreted prokineticin 2 (PK2) functions as a chemoattractant for SVZ-derived neuronal progenitors. Within the OB, PK2 may also act as a detachment signal for chain-migrating progenitors arriving from the RMS. PK2 deficiency in mice leads to a marked reduction in OB size, loss of normal OB architecture, and the accumulation of neuronal progenitors in the RMS. These findings define an essential role for G protein–coupled PK2 signaling in postnatal and adult OB neurogenesis.

In mammals, neurogenesis occurs mainly during embryonic to early postnatal stages. However, there are two areas in the adult mammalian brain that generate new neurons throughout life: OB and the dentate gyrus of the hippocampus (*1*, *2*). In rodents as well as primates, granular and periglomerular interneurons of the OB are continuously generated from SVZ of the lateral ventricle and are added throughout adulthood (*3–5*). SVZ progenitor cells migrate tangentially to the ependyma and subependymal layers of the olfactory ventricle (OV) in homotypic cell chains that coalesce to form RMS (*6–8*). Within the OB, the progenitors detach from their homotypic chains as individual cells and switch from tangential to radial migration before differentiating into interneurons of the granule and periglomerular layers (*6*, *7*). Genetic studies in mice have revealed that the polysialylated form of neural cell adhesion molecule (PSA-NCAM) is crucial for the establishment of homotypic chains of the RMS (*8–11*). Reelin and tenascin-R signaling may be involved in the dispersion of chained neuronal progenitors into single cells (*12*, *13*). Slit, a secreted repellent for axons, repels the postnatal SVZ neurons (*14*, *15*). Although a neuronal attractant from the OB has yet to be identified, diffusible attractants for SVZ neuronal progenitors may exist within layers of the OB (*16*). Here we show that prokineticin 2 (PK2) possesses features expected of a chemoattractant for SVZ-derived neuronal progenitors and is indispensable for the establishment of normal OB architecture.

Prokineticins PK1 and PK2 are cysteine-rich secreted proteins that regulate diverse biological processes by the activation of two cognate G protein–coupled receptors (*17–23*). Our analysis indicated that both prokineticin receptors (PKR1 and PKR2) are expressed in the areas active in neurogenesis during adulthood. The mRNAs of both receptors are expressed in the SVZ, the entire RMS, and the ependyma and subependymal layers of the OV, as well as the dentate gyrus of the hippocampus (Fig. 1, A to C, and figs. S1 and S12). The expression of PKR1 has detected in all these areas, although less abundantly than PKR2 (fig. S1) Whereas PK1 mRNA was not detected in any of these brain regions (*24*), PK2 has expressed in the granular and periglomerular layers of the OB (Fig. 1, D and E). The PK2 expression pattern is complementary to that of its receptors, PKR1 and PKR2; PK2 is expressed in the mature granular and periglomerular layers of the OB, whereas its receptors are expressed in the immature ependyma and subependymal layers of the OV. Similar patterns for PK2 and its receptors were observed during neonatal stages, postnatal day (P) 1, and P7 (Fig. 1, F to I; PKR1) (*24*). The expression level of PKR2 was greater during neonatal development, reflecting that the RMS forms a much thicker stream of migrating neuronal progenitors in neonates than in adults (Fig. 1, F, H, and I) (*25*). The complementary expression pattern of ligand (PK2) and receptors (PKR1 and PKR2) suggests that this ligand-receptor(s) pair may be involved

Department of Pharmacology, University of California–Irvine (UCI), Irvine, CA 92697, USA.

*To whom correspondence should be addressed. E-mail: qzhou@uci.edu

in OB neurogenesis. This hypothesis is supported by the similarities that exist between angiogenesis and neurogenesis (*26*, *27*). In particular, prokineticins can stimulate the proliferation, survival, and migration of endothelial cells derived from endocrine organs (*19*, *28*). PK2 and its receptors may serve a similar function for SVZ-derived neuronal progenitors en route to the OB during neonatal and adult stages.

To investigate whether PK2 can function as a chemoattractant for SVZ neuronal progenitors, we used a Transwell assay. Dissociated cells from the RMS and OV regions that highly expressed PKR1 and PKR2 from P7 and adult rats were placed in the upper chamber and allowed to migrate through the membrane filter separating the upper and lower chambers. Cells that migrated to the lower side of the filter were stained with Tuj1, a marker for immature neurons, and counted. When purified recombinant human PK2 (*17*) was added to the lower chamber, the migration of neuronal progenitors was enhanced (fig. S2) [P7 rat data (*24*)]. A prokineticin receptor antagonist (A1MPK1) (*29*) inhibited the PK2-stimulated cell migration (fig. S2). Thus, PK2 can stimulate the motility of neuronal progenitors from the SVZ-OB pathway. To further assess whether the PK2-stimulated cell migration is directional, coculturing experiments with the anterior portion of the SVZ (SVZa) and a stable T293 cell line expressing human PK2 were carried out in collagen gel matrices (*15*). When SVZa explants from P7 rats were cocultured with untransfected T293 cells for 24 hours, cells migrating from each explant were symmetrically distributed around its circumference (Fig. 2A). When SVZa explants were cocultured with T293 cells stably expressing human PK2, cell migration was highly asymmetric, with more cells migrating into the quadrant proximal to the PK2-expressing cells (Fig. 2B). Over time, the entire circumference of the explant showed more outwardly migrating cells, consistent with the increased motility and migration seen with the Transwell assay (fig. S3). The proximal/distal ratio of cells migrating from the SVZa-PK2 coculture was significantly higher than the control (SVZa-PK2, 3.97 ± 0.18, n = 38 explants; control, 1.05 ± 0.05, n = 23 explants; P < 0.0001) (Fig. 2D). Similar results were obtained from explants taken along the RMS (*24*). Immunocytochemistry with Tuj1 antibody confirmed the neuronal nature of the cells migrating out of the SVZa explants (fig. S4). Moreover, the addition of A1MPK1 to the collagen gel matrices in SVZa explants cocultured with PK2 T293 cells resulted in a symmetric distribution of cells (1.03 ± 0.07, n = 6 explants) and fewer migrating cells (Fig. 2, C and D). To further discern the directional nature of the PK2 signal, SVZa explants were cultured in collagen gel for 24 hours, and then control cells or PK2-expressing cell aggregates were placed nearby (*30*). A significant increase in the mean number of migrating neuronal progenitors in quadrants proximal to the PK2-expressing cells was observed (fig. S5). With SVZa-PK2 cocultures in addition to more cells migrating into the proximal quadrant, they also traveled farther away compared to controls (Fig. 2E). We also tested the motility effect of recombinant PK2 in SVZa explants by embedding it in collagen gel matrices. Figure 2F shows that PK2 increased the distance of neuronal migration; the average migration distance of individual cells in the presence of PK2 was 150.6 ± 10.5 μm versus 68.3 ± 5.8 μm in the control cultures (n = 5 explants, P < 0.0001). Taken together, these results indicate that PK2 can function as a chemoattractant for neuronal progenitors that traverse the SVZ/RMS/OB pathway.

A required step in the switch from tangential to radial migration is the detachment of neuronal progenitors from their homotypic chains. We tested whether PK2 facilitates this detachment process with matrigel (*8*). In the absence of PK2, SVZa explants showed a symmetric pattern of cell chains emanating from each explant after 24 to 30 hours in culture (Fig. 2G). These chains were either linear aggregates radiating from the explants or intricate three-dimensional networks. With recombinant PK2 embedded in the matrigel, cell chains were rarely observed and tended to be fragmented, and many cells migrated out of the explants as individuals (Fig. 2H). PK2 treatment caused a fourfold increase in the number of individual cells migrating out of explants (control, 28.9 ± 1.7, n = 40 explants; PK2-treated, 139.4 ± 5.1, n = 40 explants; P < 0.0001) (Fig. 2I). The increase in cell motility seen with PK2 treatment was also obvious with the matri-

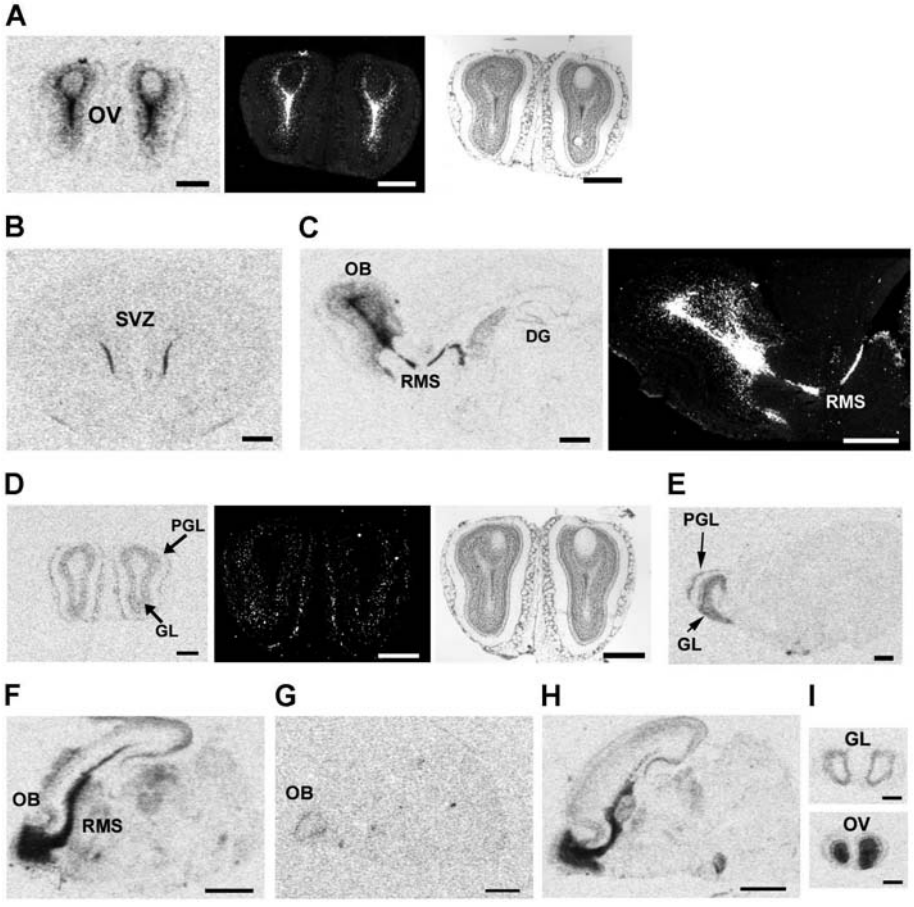

Fig. 1. PK2 and PKR2 mRNA expression. (**A**) Coronal section of adult OB, showing PKR2 (left) in the ependyma and subependymal layers of the OV, a darkfield image (middle), and cresyl violet staining (right). (**B**) PKR2 in the adult SVZ of the lateral ventricle (coronal section). (**C**) Sagittal section of an adult brain (left), depicting PKR2 in the RMS, OB, and the dentate gyrus (DG) of the hippocampus, and a darkfield image (right). (**D**) PK2 (left) in the GL and PL of adult OB, a darkfield image (middle), and cresyl violet staining (right). (**E**) Sagittal section of an adult brain, depicting PK2 in the GL and PGL. (**F**) PKR2 and (**G**) PK2 in sagittal sections of P1 brain. (**H**) Sagittal section of PKR2 in a P7 brain. (**I**) PK2 (top) and PKR2 (bottom) in coronal sections of P7 OB. Scale bar, 1 mm.

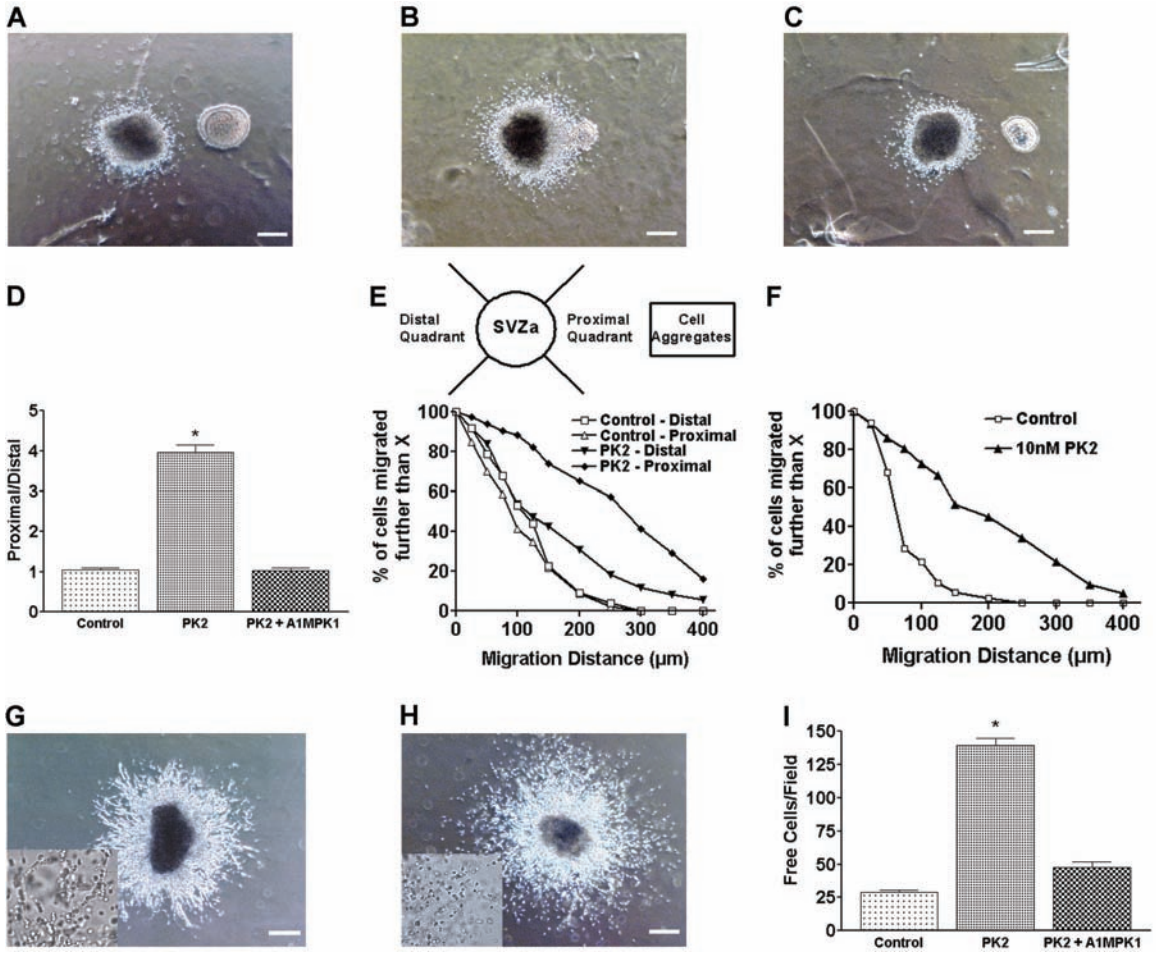

Fig. 2. Effects of PK2 on neuronal migration. (**A** to **C**) Migration of SVZa cells cocultured with (A) T293 cells, (B) the stable PK2 cell line, and (C) the PK2 stable cell line with 100-nM A1MPK1. (**D**) Proximal/distal distribution of SVZa cells in cocultures: control, PK2, or PK2 with 100-nM A1MPK1 (*, $P < 0.0001$). (**E**) Migration distances of SVZa cells with control cells or the PK2 stable cell line. The *x* axis shows the distance of cells from SVZa explants; the *y* axis, the percentage of cells that migrated further than the distance on the *x* axis. Values shown are representative of three independent experiments. (**F**) Increased motility of SVZa cells in collagen embedded with 10-nM PK2 versus control cells at 24 hours. Values shown are representative of five independent experiments. (**G**) Chains of cells migrating from SVZa explant cultured alone in matrigel. (Inset) Higher magnification of (G). (**H**) Dispersal of cells from SVZa explant cultured with 60-nM PK2. (**Inset**) Higher magnification of (H), highlighting changes in cellular organization. (**I**) Quantification of distinguishable individual cells per visual field, in matrigel cultures with either 60-nM PK2 or 60 nM PK2 and 120-nM A1MPK1 (*, $P < 0.0001$). Scale bar, 500 μm.

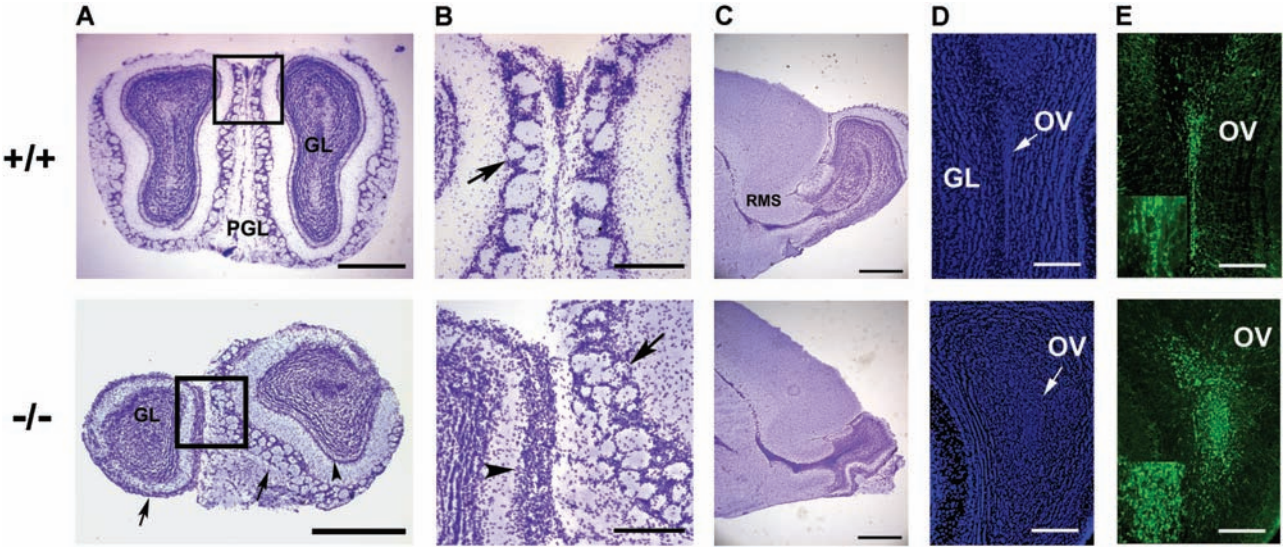

Fig. 3. Analysis of olfactory bulbs from $PK2^{-/-}$ mice. (**A**) Nissl-stained coronal section of WT (top) and $PK2^{-/-}$ OB (bottom). GL and PGL (arrows) are disorganized in $PK2^{-/-}$ OB. The arrowhead shows the mitral cell layer. (**B**) Magnification of the PGL (box) in (A). The top panel shows normal PGL (arrow) in WT OB; the bottom shows, in $PK2^{-/-}$ OB, abnormal glomeruli formation (arrow) and a single uninterrupted PGL (arrowhead). (**C**) Nissl-stained sagittal sections of WT (top) and $PK2^{-/-}$ (bottom) brain. (**D**) 4′, 6-diamidino-Z-phenylindole-stained (blue) coronal sections of WT (top) and $PK2^{-/-}$ OB (bottom). (**E**) Sections in (D) immunostained for PSA-NCAM (green). The top panel shows PSA-NCAM–labeled neuronal progenitors in the OV of WT OB. (Top inset) A higher magnification of the top panel shows normal OV. The bottom panel shows an expanded OV with accumulation of neuronal progenitors in $PK2^{-/-}$ OB. (Bottom inset) A higher magnification of the bottom panel shows tight clusters of PSA-NCAM–labeled neuronal progenitors in the OV. Scale bars, 1 mm in (A) and (C); 250 μm in (B), (D), and (E).

gel cultures (Fig. 2, G and H). Moreover, the separation of individual cells in PK2-treated cultures was reduced with the addition of the antagonist A1MPK1 (Fig. 2I). Thus, PK2 may act as a detachment signal for neuronal progenitors migrating within the chain.

In mutant mice deficient in the PK2 gene ($PK2^{-/-}$ mice) (*31*), the total weight and gross morphology of brains did not differ from those of wild-type (WT) controls, but the size of their OBs was less than half that of the WT controls (rostral to caudal length: 3.68 ± 0.09 mm versus 1.27 ± 0.11 mm, WT versus $PK2^{-/-}$, respectively, $n = 20$ mice, $P < 0.0001$; weight: 7.67 ± 0.33 mg versus 16.67 ± 1.45 mg, $PK2^{-/-}$ versus WT, respectively, $n = 3$ mice, $P < 0.005$) (fig. S6). Although OBs from $PK2^{-/-}$ mice were smaller than those from WT controls in all cases, ~50% of $PK2^{-/-}$ mice displayed asymmetric bulb formation (fig. S6A). Histological examination revealed multiple abnormalities of the OB from $PK2^{-/-}$ mice (Fig. 3, A to C). Whereas the mitral cell layer appeared normal in the OB of $PK2^{-/-}$ mice, the granular cell layer (GL) was abnormally thin (fig. S6B), and the number of granular cells was reduced (*24*). The periglomerular layer (PGL) was either indiscernible or malformed in $PK2^{-/-}$ mice (Fig. 3, A to C). In contrast, the small OBs in NCAM-deficient mice have a normal PGL (*10*). In 16 of the 28 OBs examined in $PK2^{-/-}$ mice, the PGL was not discernable and was replaced by an uninterrupted layer of periglomerular cells (Fig. 3B). In the remaining OBs examined, multiple glomeruli layers were compacted on a single side of the OB (Fig. 3B). The PGL possesses a population of dopaminergic (DA) interneurons born from the SVZ-OB pathway (*32*). Immunostaining for tyrosine hydroxylase (TH), a marker for these interneurons, in the OB of $PK2^{-/-}$ mice that had no discernable PGL was minimal, whereas collectively there was a fourfold reduction in DA interneurons in the PGL compared to that of WT controls (102.7 ± 16.4 TH^+ cells/mm² versus 24.7 ± 20.2 TH^+ cells/mm², WT versus $PK2^{-/-}$, respectively; $n = 3$ mice, $P < 0.05$) (fig. S7).

The smaller OB in $PK2^{-/-}$ mice was accompanied by a significant enlargement of both the OV and the RMS at the entrance of OB (Fig. 3C and fig. S8). Immunostaining for chains of neuronal progenitors with PSA-NCAM demonstrated the accumulation of neuronal progenitors around the OV in $PK2^{-/-}$ mice (Fig. 3, D and E). PSA-NCAM–positive cells clustered tightly around the OV in the $PK2^{-/-}$ mice (Fig. 3, D and E). The accumulation of neuronal progenitors in the rostral portion of the RMS and OV and a layer specific reduction in a subset of interneurons derived from the SVZ suggests that cell migration was initiated but compromised in the OB in $PK2^{-/-}$ mice.

The normal distribution and density of bromodeoxyuridine-labeled ($BrdU^+$) cells in the SVZ and RMS in $PK2^{-/-}$ mice indicates that the smaller OB is not due to reduced cell proliferation (fig. S9). A pulse of BrdU was used to trace the migration of neuronal progenitors through the SVZ-OB pathway however revealed differences between WT and $PK2^{-/-}$ mice (Fig. 4, A and B). Five days after the pulse in $PK2^{-/-}$ mice, $BrdU^+$ cells accumulated abnormally in the RMS outside the OB (Fig. 4E and fig. S10) and in the OV (Fig. 4, A, B, and E) (551.3 ± 56.7 versus 969.1 ± 129.5 $BrdU^+$ cells/mm² in the RMS outside of the OB and 867.6 ± 139.8 versus 1571 ± 142.0 $BrdU^+$ cells/mm² in the OV for WT and $PK2^{-/-}$ mice, respectively; $n = 3$ mice, $P < 0.05$). At 28 days after the pulse in WT mice, most $BrdU^+$ cells were found in the rostral half of the OB integrated into the GL and PGL (Fig. 4, C and D). In $PK2^{-/-}$ mice, $BrdU^+$ cells in the OB were reduced (128.9 ± 9.0 $BrdU^+$ cells/mm² versus 50.2 ± 2.8 $BrdU^+$ cells/mm², WT versus $PK2^{-/-}$, respectively; $n = 3$ mice, $P < 0.001$) (Fig. 4, C, D, and F), and most of these $BrdU^+$ cells were found at the entrance of the OB and in the OV. The distribution of $BrdU^+$ cells suggests that the accumulation of neuronal progenitors in the OV of $PK2^{-/-}$ mice might lead to a higher rate of cell death within the OB. Terminal deoxynucleotidyl transferase mediated–deoxyuridine triphosphate UTP nick-end labeling (TUNEL) analysis indicated increased apoptosis in the OB of $PK2^{-/-}$ mice (6.8 ± 2.2 $TUNEL^+$ cells/mm² versus 27.9 ± 5.9 $TUNEL^+$ cells/mm², WT versus $PK2^{-/-}$, respectively; $n = 3$ mice, $P < 0.05$) (fig. S11). These observations are consistent with the marked buildup

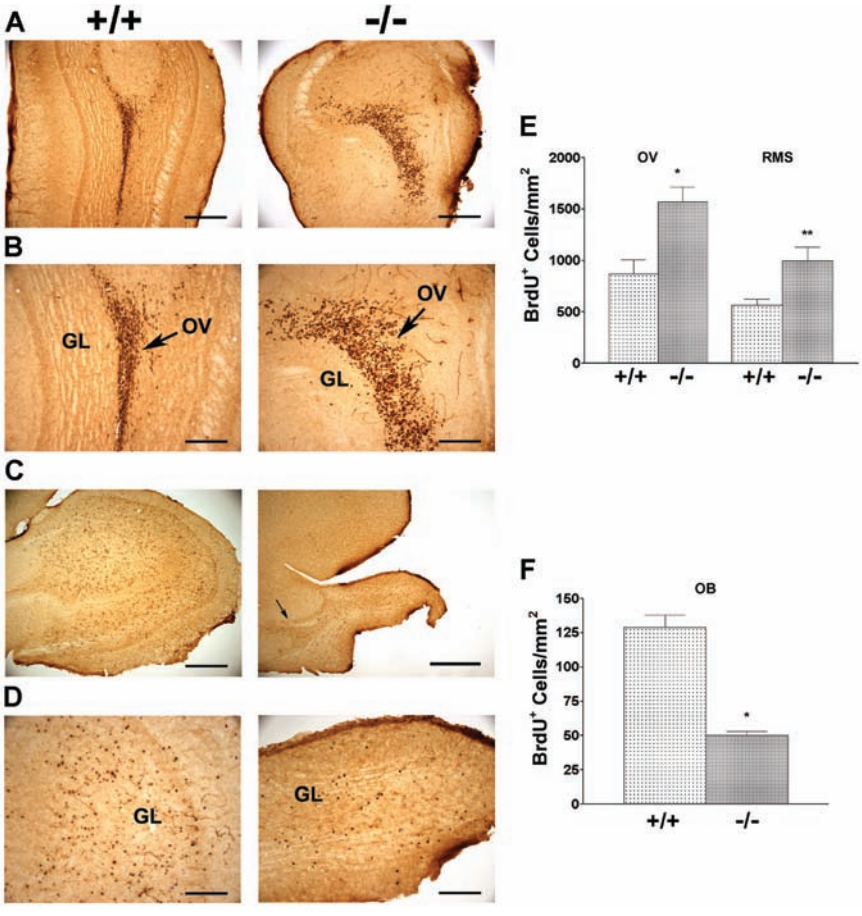

Fig. 4. Migration of neuronal progenitors in $PK2^{-/-}$ mice. (**A**) Coronal section of WT OB 5 days after pulse injection of BrdU, showing (left) diaminobenzidine-stained $BrdU^+$ cells in the OV and (right) increased $BrdU^+$ cells around the OV in $PK2^{-/-}$ OB. (**B**) Higher magnifications of (A), showing a wider OV in $PK2^{-/-}$ OB (right). (**C**) Sagittal section of WT OB 28 days after a pulse of BrdU, showing (left) numerous $BrdU^+$ cells. $PK2^{-/-}$ OB (right) shows a reduction of $BrdU^+$ cells and accumulation near the entrance of the OB (arrow). (**D**) High magnification showing numerous $BrdU^+$ cells in the GL and the PGL in WT OB (left). In $PK2^{-/-}$ OB (right), $BrdU^+$ cells were reduced and around the OV and GL. (**E**) Quantification of $BrdU^+$ cells in the OV and RMS from the 5-day pulse study (* and **, $P < 0.05$). (**F**) Quantification of $BrdU^+$ cells in the OB from the 28-day pulse study (*, $P < 0.001$). Scale bars, 500 μm in (C); 250 μm in (A); 125 μm in (B) and (D).

of PKR2-positive cells in the rostral portion of the RMS and OV of PK2$^{-/-}$ mice (fig. S12), also shown by PSA-NCAM immunostaining (Fig. 3E). Analysis of PKR2 mRNA expression in PK2$^{-/-}$ mice showed an overall decrease in neuronal progenitors migrating away from the OV into the GL and PGL (fig. S12). The compaction of PKR2-positive cells in the OV indicates that, in the absence of PK2 signaling, chained neuronal progenitors are either not detached properly or disoriented about the direction of migration. To evaluate whether PK2 is a genuine chemoattractant for SVZ neuronal progenitors, we performed SVZa explants coculture assay with the GL of the OB, where PK2 is primarily expressed (Fig. 1, D and E). Cell migration was directed toward the GL tissue from WT OB, whereas the corresponding tissue from PK2$^{-/-}$ OB exhibited no chemotaxis activity (proximal/distal ratio: 1.87 ± 0.31 versus 0.99 ± 0.06, WT versus PK2$^{-/-}$, respectively; $n = 6$ explants, $P < 0.05$) (fig. S13). Taken together, these results indicate that the migration of neuronal progenitors mediated by PK2 signaling is essential for the normal development and maintenance of the OB.

Thus, PK2 serves as a chemoattractant for SVZ-derived neuronal progenitors, and the establishment of normal OB architecture requires PK2 signaling. Together with other signals (*12*, *13*, *15*), PK2 appears to guide the migration of neuronal progenitors from the SVZ through the RMS to their final layers in the OB. The similar response of PKR1 and PKR2 to PK2 (*22*) implies that these receptors may mediate a redundant role for OB development. As with endothelin-3 signaling for the migration of enteric neurons (*33*) and orphan receptor GPR56 in the regional development of the cerebral cortex (*34*), our results further indicate that G protein–coupled receptors may be crucial for the establishment of the layered structures in the nervous system.

References and Notes

1. J. Altman, *J. Comp. Neurol.* **137**, 433 (1969).
2. F. H. Gage, *Science* **287**, 1433 (2000).
3. M. S. Kaplan, J. W. Hinds, *Science* **197**, 1092 (1977).
4. S. A. Bayer, *Exp. Brain Res.* **50**, 329 (1983).
5. V. Pencea, K. D. Bingaman, L. J. Freedman, M. B. Luskin, *Exp. Neurol.* **172**, 1 (2001).
6. M. B. Luskin, *Neuron* **11**, 173 (1993).
7. C. Lois, A. Alvarez-Buylla, *Science* **264**, 1145 (1994).
8. H. Wichterle, J. M. Garcia-Verdugo, A. Alvarez-Buylla, *Neuron* **18**, 779 (1997).
9. H. Tomasiewicz *et al.*, *Neuron* **11**, 1163 (1993).
10. H. Cremer *et al.*, *Nature* **367**, 455 (1994).
11. K. Ono, H. Tomasiewicz, T. Magnuson, U. Rutishauser, *Neuron* **13**, 595 (1994).
12. I. Hack, M. Bancila, K. Loulier, P. Carroll, H. Cremer, *Nat. Neurosci.* **5**, 939 (2002).
13. A. Saghatelyan, A. de Chevigny, M. Schachner, P. M. Lledo, *Nat. Neurosci.* **7**, 347 (2004).
14. H. Hu, U. Rutishauser, *Neuron* **16**, 933 (1996).
15. W. Wu *et al.*, *Nature* **400**, 331 (1999).
16. G. Liu, Y. Rao, *J. Neurosci.* **23**, 6651 (2003).
17. M. Li, C. M. Bullock, D. J. Knauer, F. J. Ehlert, Q. Y. Zhou, *Mol. Pharmacol.* **59**, 692 (2001).
18. M. Y. Cheng *et al.*, *Nature* **417**, 405 (2002).
19. J. LeCouter *et al.*, *Proc. Natl. Acad. Sci. U.S.A.* **100**, 2685 (2003).
20. C. Mollay *et al.*, *Eur. J. Pharmacol.* **374**, 189 (1999).
21. L. Negri *et al.*, *Br. J. Pharmacol.* **137**, 1147 (2002).
22. D. C. Lin *et al.*, *J. Biol. Chem.* **277**, 19276 (2002).
23. T. Soga *et al.*, *Biochim. Biophys. Acta* **1579**, 173 (2002).
24. K. L. Ng *et al.*, unpublished data.
25. K. Kishi *et al.*, *Arch. Histol. Cytol.* **53**, 219 (1990).
26. H. Zhang, L. Vutskits, M. S. Pepper, J. Z. Kiss, *J. Cell Biol.* **163**, 1375 (2003).
27. T. D. Palmer, A. R. Willhoite, F. H. Gage, *J. Comp. Neurol.* **425**, 479 (2000).
28. J. LeCouter *et al.*, *Nature* **412**, 877 (2001).
29. C. M. Bullock, J. D. Li, Q. Y. Zhou, *Mol. Pharmacol.* **65**, 582 (2004).
30. M. Ward, C. McCann, M. DeWulf, J. Y. Wu, Y. Rao, *J. Neurosci.* **23**, 5170 (2003).
31. J. D. Li *et al.*, unpublished data.
32. R. Betarbet, T. Zigova, R. A. Bakay, M. B. Luskin, *Int. J. Dev. Neurosci.* **14**, 921 (1996).
33. A. G. Baynash *et al.*, *Cell* **79**, 1277 (1994).
34. X. Piao *et al.*, *Science* **303**, 2033 (2004).

35. We thank H. van Praag, O. Steward, and C. Zhang for discussions; C. Tu and H. Shen for technical assistance; and the laboratories of C. Cotman and F. LaFerla for access to equipment. Supported by a University of California Discovery grant. K.N. is a recipient of a UCI Medical Scientist Training Program training grant.

Supporting Online Material
www.sciencemag.org/cgi/content/full/308/5730/1923/DC1
Materials and Methods
Figs. S1 to S13
References and Notes

10 March 2005; accepted 2 May 2005
10.1126/science.1112103

GDF11 Controls the Timing of Progenitor Cell Competence in Developing Retina

Joon Kim,[1,2] Hsiao-Huei Wu,[1,2]* Arthur D. Lander,[2,3] Karen M. Lyons,[4] Martin M. Matzuk,[5] Anne L. Calof[1,2]†

The orderly generation of cell types in the developing retina is thought to be regulated by changes in the competence of multipotent progenitors. Here, we show that a secreted factor, growth and differentiation factor 11 (GDF11), controls the numbers of retinal ganglion cells (RGCs), as well as amacrine and photoreceptor cells, that form during development. GDF11 does not affect proliferation of progenitors—a major mode of GDF11 action in other tissues—but instead controls duration of expression of *Math5*, a gene that confers competence for RGC genesis, in progenitor cells. Thus, GDF11 governs the temporal windows during which multipotent progenitors retain competence to produce distinct neural progeny.

The vertebrate neural retina comprises seven neural cell types, all derived from one population of multipotent progenitors (*1*, *2*). Retinal cell types do not arise synchronously but are generated in a stereotyped sequence (*3*, *4*). In vitro results imply that retinal progenitors at different stages differ in their competence to produce distinct cell types (*5*–*7*). Such changes in potential are likely dictated by changes in expression of the transcription factors encoded by proneural genes (*8*, *9*), but mechanisms of proneural gene regulation are poorly understood. An important role for cell-cell signaling is suggested by the fact that production of at least two retinal cell types, retinal ganglion cells (RGCs) and amacrine cells, can increase to compensate for losses of mature cells in either population (*10*, *11*). This process has been postulated to be mediated by a feedback signal produced by mature cells (*12*), but the identity of the signal(s) is unknown.

GDF11, a member of the transforming growth factor-β superfamily of secreted signaling molecules, is expressed in several regions of a developing nervous system, including the retina (*13*). In olfactory epithelium (OE), GDF11 negatively regulates neuron number by causing cell-cycle arrest of the progenitor cells that give rise to olfactory receptor neurons (ORNs) (*14*). Here, we demonstrate that GDF11 is also a negative regulator of neuron number in neural retina, but through a completely different mechanism: GDF11 controls

[1]Department of Anatomy and Neurobiology, [2]Developmental Biology Center, [3]Department of Developmental and Cell Biology, University of California, Irvine, CA 92697, USA. [4]Department of Molecular, Cell, and Developmental Biology, University of California, Los Angeles, CA 90095, USA. [5]Department of Molecular and Human Genetics, Baylor College of Medicine, Houston, TX 77030, USA.

*Present address: Department of Biochemistry, Vanderbilt University, Nashville, TN 37232, USA.
†To whom correspondence should be addressed. Email: alcalof@uci.edu